1986

Parallel Plate Electrochemical Reactor Model: Material Balance Closure and a Simplification

M J. Mader
Texas A & M University - College Station

C W. Walton
Texas A & M University - College Station

Ralph E. White
University of South Carolina - Columbia, white@cec.sc.edu

Publication Info

Parallel Plate Electrochemical Reactor Model: Material Balance Closure and a Simplification

M. J. Mader, C. W. Walton,* and R. E. White**

Department of Chemical Engineering, Texas A&M University, College Station, Texas 77843

ABSTRACT

A material balance closure calculation is presented to test the consistency of a previously published model of a parallel plate electrochemical reactor. New expressions are used in this procedure to calculate the average concentration of species i and the average current density for reaction j from the predicted concentration and potential distributions. Also, the previously presented model equations are simplified by assuming that the axial concentration gradient for species i can be approximated by a step change from the known feed concentration to the unknown outlet concentration. This one-step model provides a qualitative evaluation of cell performance and adds insight into understanding of the previous model, while providing substantial savings in computer time. The models are compared using a hypothetical case of the electrowinning of copper from a chloride solution. For a small aspect ratio (S/L), the models show that a set of independent variables consists of the cell potential (E_{cell}), the surface area of an electrode per unit of cell volume ($1/S$), and the residence time (L/v_{avg}) when the feed concentrations ($c_{i,feed}$) are fixed.

White, Bain, and Raible [1] presented a model of a parallel plate electrochemical reactor with multiple electrode reactions which can be used to predict such quantities as current efficiencies and conversion per pass under various cell conditions. This information is valuable in the design of both bench and production scale parallel plate cells and in the selection of operating conditions to use for optimum performance. The model of White et al. [1] is a "complete" model in the sense that the interaction between closely spaced electrodes is included in the model equations, multiple electrode reactions can occur, and predictions of cell performance such as the conversion per pass are made. Their model is an alternative to the less complete models of Sakellaropolous and Francis [2-4], Parrish and Newman [5], Caban and Chapman [6], and Lee and Selman [7]. Sakellaropolous and Francis [2-4] presented a model for a parallel plate cell which has multiple reactions at one electrode, but their model does not include the effect of the cell gap (S). Parrish and Newman [5] presented a model which takes the interaction of closely spaced electrodes into account, but they did not include multiple electrode reactions. Caban and Chapman [6] presented essentially the same model as Parrish and Newman [5] except that they set the cell potential instead of the cell current. Lee and Selman [7] presented a model of the Zn/Br_2 cell, but did not include multiple electrode reactions. This paper presents corrections to and a simplified version of the earlier model [1]. Specifically, an alternate form for calculating the local average concentration of species i [$c_{i,avg}(x)$] is derived, and a check for material balance closure of the model is presented. This is followed by the development of an approximate, "one-step" model. Finally, sets of dimensionless and dimensional groups are presented that can be used to predict the performance of the cell. Following these developments, the results of each are discussed in regard to a hypothetical case of the electrowinning of copper from a chloride solution.

Developments

White et al. [1] describe a two-dimensional model of a parallel plate electrochemical reactor with multiple electrode reactions under laminar flow. As published, there are minor errors in that paper. Specifically, Eq. [12] of Ref. [1] should include an α multiplying the left-hand side of the equation and a θ_i multiplying the term $\partial^2\Phi/\partial\eta^2$ on the right-hand side. Also, the reference concentration for Cl^- in their Table I should have been listed as 0.1 instead of 1.0 and the exchange current density column heading should have been $10^5 \cdot i_{oj,ref}$ instead of $10^8 \cdot i_{oj,ref}$.

As shown in the cell schematic of Fig. 1, the concentration of each species in the solution (c_i) and the potential of the solution (Φ) depend on the coordinates x and y. Consequently, the current density of reaction j (i_{nj}) is also a function of axial position. The governing nonlinear partial differential equations and boundary conditions are solved using an implicit stepping technique [8] in the axial direction and Newman's BAND algorithm [9, 10] in the radial direction. The BAND algorithm is used to determine c_i and Φ at a specific value of x, then, a step of size Δx is taken in the axial direction and the set of variables is calculated again using the BAND algorithm. This stepwise procedure is repeated until $x = L$.

The mathematical definition of what White et al. [1] call bulk average concentration, $c_{i,avg}(x)$, is improper if one wishes to determine a conversion per pass of a particular species and thus causes problems in achieving a material balance using the model's predicted concentration profile. The definition used by White et al. [1] for $c_{i,avg}$ [see Eq. [32] of Ref. [1]] is incorrect because the velocity profile between the plates is laminar and not plug flow. Thus, it is appropriate to calculate what might best be termed a local average concentration by beginning with a radial average of the molar flux of a species at a particular value of x. This is given by

$$N_{fi,avg}(x) = \frac{1}{S}\int_0^S N_{fi}(x, y)\, dy \qquad [1]$$

where $N_{fi}(x, y)$ is the molar flux in the flow direction and is expressed as

$$N_{fi}(x, y) = -D_i\frac{\partial c_i}{\partial x} - \frac{z_i D_i \mathbf{F}}{RT} c_i \frac{\partial \Phi}{\partial x} + v_x c_i \qquad [2]$$

Since it is assumed that the electrode length (L) is much greater than the electrode gap (S), the aspect ratio ($\alpha = S/L$) is small and therefore migration and diffusion in the axial (flow) direction are negligible compared to forced convection, as shown in more detail by Nguyen et al. [11]. In this case, $N_{fi,avg}$ may be replaced by $v_{avg}c_{i,avg}(x)$ and $N_{fi}(x, y)$ may be replaced by $v_x c_i$ in Eq. [1]. Under well-developed laminar flow, the velocity profile is given by

$$v_x(y) = 6v_{avg}\left(\frac{y}{S} - \frac{y^2}{S^2}\right) \qquad [3]$$

and Eq. [1] can be solved for the local average concentration to give

$$c_{i,avg}(x) = \frac{6}{S}\int_0^S \left(\frac{y}{S} - \frac{y^2}{S^2}\right) c_i(x, y)\, dy \qquad [4]$$

If the dimensionless variables used by White et al. [1] are introduced, Eq. [4] becomes

$$\theta_{i,avg}(\zeta) = 6\int_0^1 (\eta - \eta^2)\theta_i(\zeta, \eta)\, d\eta \qquad [5]$$
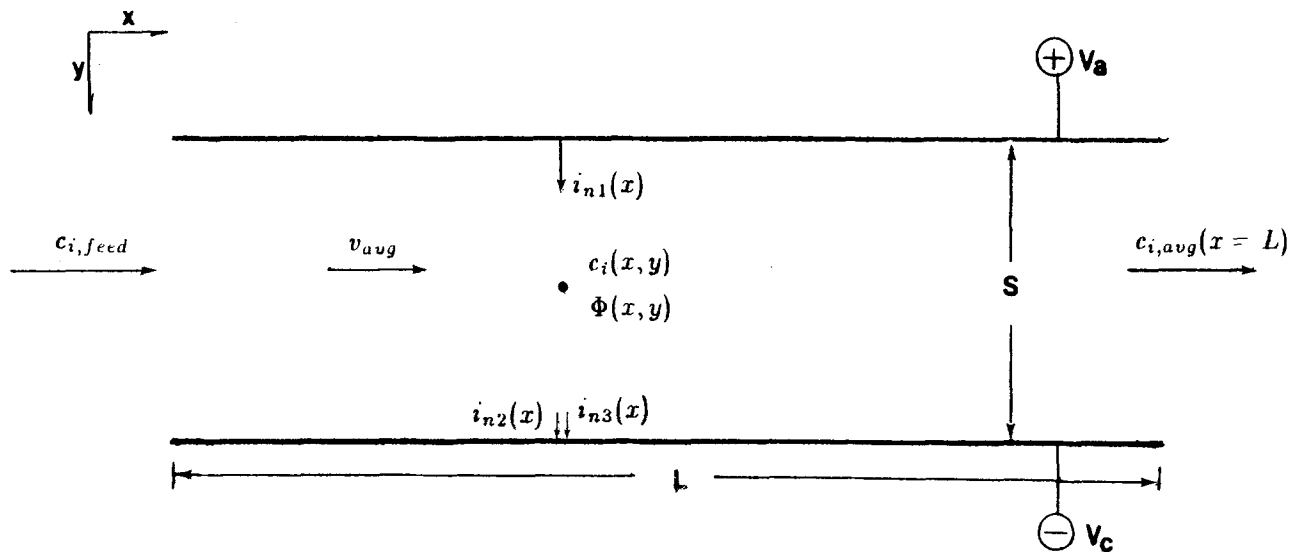
1124

Fig. 1. Schematic of a simple parallel plate electrochemical reactor

where

$$\zeta = x/L \qquad [6]$$

$$\eta = y/S \qquad [7]$$

and

$$\theta_i = c_i/c_{i,ref} \qquad [8]$$

The integral in Eq. [5] can be evaluated by an appropriate numerical method, such as Simpson's rule, based on the concentrations calculated for each radial step at a fixed axial position.

The consistency of the model can be verified by using the calculated concentration profiles to obtain a material balance closure over the parallel plate reactor for species i. The net rate of consumption by all of the electrochemical reactions occurring on both electrodes for species i in mol/s is

$$\begin{array}{l} \text{net rate of} \\ \text{consumption of species} = \\ \text{i by all electro-} \\ \text{chemical reactions} \end{array} \sum_{j=1}^{nr} \frac{s_{ij} i_{nj,avg}}{n_j F} LW$$

where s_{ij} is the stoichiometric coefficient for species i in electrode reaction j (s_{ij} is positive if i is an anodic reactant and negative if i is a cathodic reactant), LW is the area of each electrode, and nr is the total number of electrochemical reactions that occur in the cell. The rates of input and output by transport are $SWN_{fi,feed}$ and $SWN_{fi,avg}(x = L)$, respectively, where SW is the cross-sectional flow area. Since the model is for steady-state conditions, no accumulation term is necessary and the final material balance equation is

$$SW(N_{fi,feed} - N_{fi,avg}(x = L))$$

$$- \sum_{j=1}^{nr} \frac{s_{ij} i_{nj,avg}}{n_j F} LW = 0 \qquad [9]$$

Again assuming that forced convection is much greater than migration or diffusion in the axial direction, N_{fi} may be simplified so that Eq. [9] becomes

$$\sum_{j=1}^{nr} \frac{s_{ij} i_{nj,avg}}{n_j F} = [c_{i,feed} - c_{i,avg}(x = L)] \frac{v_{avg} S}{L} \qquad [10]$$

Note that each side of Eq. [10] can be calculated separately from the model results (predicted c_i and Φ) and compared for consistency.

Since the model presented by White *et al.* (1) requires substantial computing time, a simplified model was developed that can be used to obtain approximate values for the derived quantities of interest (*e.g.*, conversion per pass) using substantially less computer time. This model can then be used to narrow the range of operating conditions that produce optimal results. The simplified model proposed here utilizes only one calculation in the flow (or axial) direction. In effect, this requires the assumption that i_{nj} is a constant along the length of the reactor and therefore, as shown schematically in Fig. 2, i_{nj} is no longer a function of x. Similarly, c_i and Φ are functions of y only. To distinguish the two models, the model of White *et al.* (1) is called the continuous model, while the simplified version is called the one-step model.

To implement this idea, the axial concentration gradient of species i in the governing equation of the continuous model [see Eq. [6] of Ref. (1)] is approximated by a step change

$$\frac{\partial c_i}{\partial x} \cong \frac{c_i(x = L, y) - c_{i,feed}}{L} \qquad [11]$$

Using the previously given dimensionless variables (Eq. [6]-[8]), Eq. [11] becomes

$$\frac{\partial \theta_i}{\partial \zeta} \cong \frac{\theta_i(\zeta = 1, \eta) - \theta_{i,feed}}{1} \qquad [12]$$

This approximation of the gradient can be substituted into Eq. [13] of White *et al.* (1)

$$3 \frac{D_R}{D_i} Pe\alpha (\eta - \eta^2) \frac{\partial \theta_i}{\partial \zeta} = \frac{\partial^2 \theta_i}{\partial \eta^2}$$
$$+ \frac{z_i F}{RT} \left[\theta_i \frac{\partial^2 \Phi}{\partial \eta^2} + \frac{\partial \theta_i}{\partial \eta} \frac{\partial \Phi}{\partial \eta} \right] \qquad [13]$$

to achieve the governing equation for the one-step model that applies at $\zeta = 1$

$$3 \frac{D_R}{D_i} Pe\alpha (\eta - \eta^2) (\theta_i - \theta_{i,feed})$$
$$= \frac{\partial^2 \theta_i}{\partial \eta^2} + \frac{z_i F}{RT} \left[\theta_i \frac{\partial^2 \Phi}{\partial \eta^2} + \frac{\partial \theta_i}{\partial \eta} \frac{\partial \Phi}{\partial \eta} \right] \qquad [14]$$

All inlet and boundary conditions, and the electroneutrality condition as discussed by White *et al.* (1) are the same for this one-step model. That is, the inlet conditions are

$$\text{at} \quad \zeta = 0m \quad \theta_i = \theta_{i,feed} \quad \text{and} \quad \sum_i z_i c_{i,ref} \theta_{i,feed} = 0 \qquad [15]$$
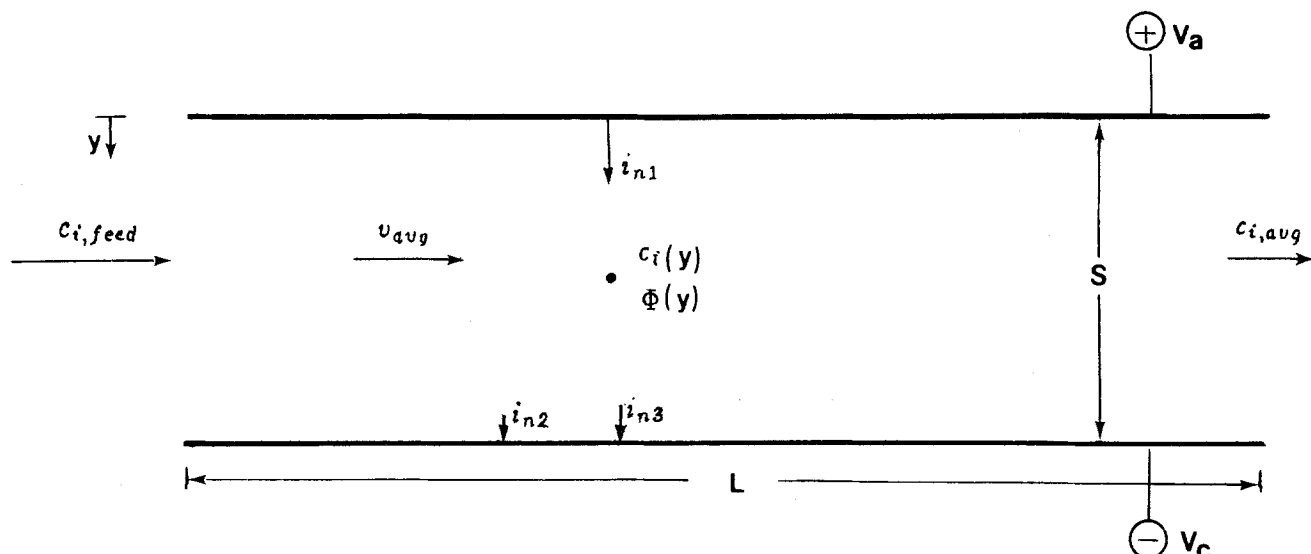
and the boundary conditions are

$$\text{for } \zeta > 0$$

Fig. 2. Schematic of the one-step model

at $\eta = 0$ (anode): $\displaystyle\sum_j \frac{s_{ij} i_{nj}}{n_j F} = -N_{ni}$ [16]

at $\eta = 1$ (cathode): $\displaystyle\sum_j \frac{s_{ij} i_{nj}}{n_j F} = N_{ni}$ [17]

and

at $\eta = 0$ and $\eta = 1$: $\displaystyle\sum_i z_i c_{i,ref} \theta_i = 0$ [18]

The governing equations and boundary conditions for the one-step model are solved by the same method as before (1).

Since the one-step model is essentially a one-dimensional model, it is a less accurate solution than the continuous model for systems with a high conversion per pass. However, it is reasonably accurate for low conversions per pass (12, 13) and its development is useful in understanding the continuous model better. Figure 3 shows schematically how the continuous model may be thought of as a series of one-step models in which concentration, potential, and, consequently, the current density of reaction j are functions of an increment of size Δx, the size of one step. Thus, the continuous model consists of a large number of one-step models using the radial concentration profile from the previous one-step model segment as the feed to the next one-step model segment with a step size Δx small enough to give results to a desired accuracy.

The calculation of the average current density of reaction j, $i_{nj,avg}$, is a good example of the importance of the

conceptualization of the continuous model as a series of one-step models. White et al. (1) give the following formula for $i_{nj,avg}$ for the continuous model

$$i_{nj,avg} = \frac{1}{L} \int_0^L i_{nj}(x)\, dx \qquad [19]$$

The correct value for $i_{nj,avg}$ for use in the material balance closure equation (Eq. [10]) could be obtained from Eq. [19] by using Simpson's rule, e.g., if a large number of steps were used to obtain $i_{nj}(x)$. However, since the solution method used here treats the concentration and potential distributions and, therefore, $i_{nj}(x)$ as constants over the previous axial step, a simple average of the $i_{nj}(x)$ values over the length L of the reactor yields an average current density that is consistent with the solutions obtained for the average exit concentrations from each step. That is, the proper expression to use to calculate the average current density to be used in the material balance closure equation (Eq. [10]) is

$$i_{nj,avg} = \frac{1}{L} \sum_{k=1}^{nk} i_{nj}(k)\, (\Delta x)_k \qquad [20]$$

where $i_{nj}(k)$ is the current density of reaction j over the kth interval. A comparison of the two methods is presented below.

Finally, for both the continuous and one-step models, it is important to identify a set of independent variables which can be used to describe the behavior of the electrochemical reactor. The variable parameters in these models are v_{avg}, S, L, and E_{cell}, with the values of $c_{i,feed}$ set equal
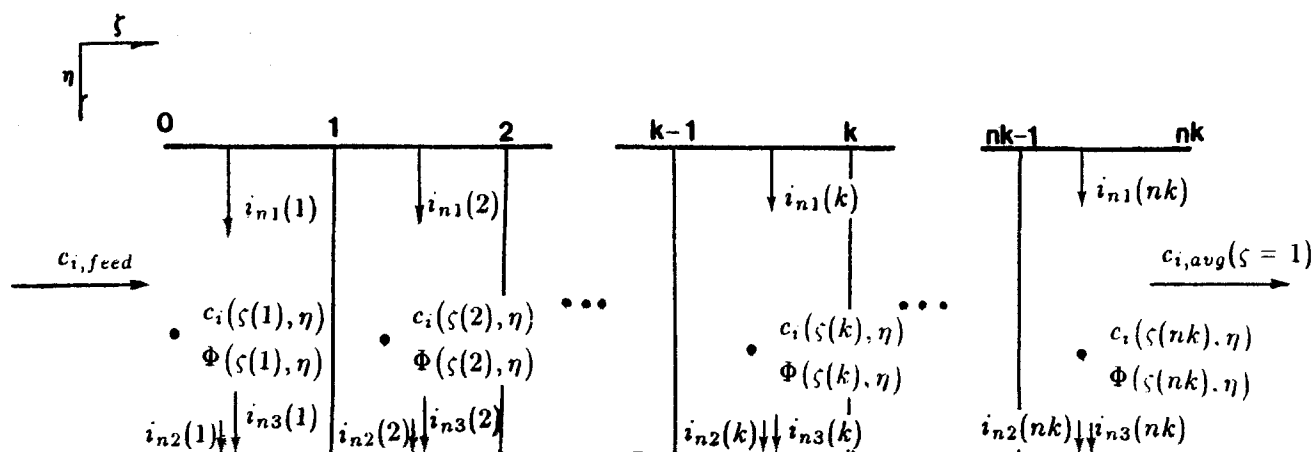

Fig. 3. Schematic of the stepwise calculation for the continuous model

to $c_{i,ref}$. Nguyen et al. (11) showed that v_{avg}, S, and L are not all independent variables. They did this by showing that for small values of the aspect ratio ($\alpha = S/L$) these variables can be combined into two dimensionless groups

$$Pe\alpha = \frac{2Sv_{avg}}{D_R}\frac{S}{L} \qquad [21]$$

and

$$\xi_{ij} = \left| \frac{s_{ij}i_{oj,ref}S}{n_j c_{i,ref}D_i\mathbf{F}} \right| \qquad [22]$$

with i and j specified appropriately (e.g., the limiting reactant in a particular reaction). These two dimensionless groups can be combined to form a different dimensionless group as follows
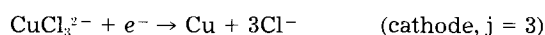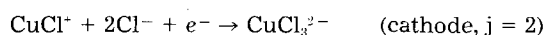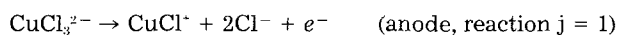
$$\beta_{ij} = \frac{\xi_{ij}^2}{Pe\alpha} = \frac{\left| \dfrac{s_{ij}i_{o,j,ref}S}{n_j c_{i,ref}D_i\mathbf{F}} \right|^2}{\dfrac{2Sv_{avg}}{D_R}\dfrac{S}{L}} \qquad [23]$$

$$\beta_{ij} = \frac{s_{ij}^2 i_{oj,ref}^2 D_R L}{2n_j^2 c_{i,ref}^2 D_i^2 \mathbf{F}^2 v_{avg}} \qquad [24]$$

Only two of these three dimensionless groups (Peα, ξ_{ij}, and β_{ij} for i and j specified properly) are independent. Consideration of ξ_{ij} and β_{ij} reveals that $1/\xi_{ij}$ could be considered to be a dimensionless surface area of an electrode per unit volume ($1/S$) and β_{ij} a dimensionless residence time (L/v_{avg}) since all of the other quantities in the expressions for ξ_{ij} and β_{ij} are considered here to be fixed. Consequently, $1/S$ and L/v_{avg} can be used as dimensional independent variables, as done here.

Results and Discussion

The developments presented above have been evaluated by using the same hypothetical case of the electrowinning of copper from a chloride solution used by White et al. (1), which should be consulted for values of the fixed parameters. The reactions considered are

$CuCl_3^{2-} \rightarrow CuCl^+ + 2Cl^- + e^-$ (anode, reaction j = 1)

$CuCl^+ + 2Cl^- + e^- \rightarrow CuCl_3^{2-}$ (cathode, j = 2)

$CuCl_3^{2-} + e^- \rightarrow Cu + 3Cl^-$ (cathode, j = 3)

Case studies have been used to test the consistency of the models by material balance closure, to compare the one-step and continuous models, and to illustrate the importance of the three independent variables ($1/S$, L/v_{avg}, and E_{cell}).

The consistency of the models is verified by use of the material balance closure relation given by Eq. [10]. The Appendix gives the details of a sample calculation based on $CuCl_3^{2-}$ for the continuous model, where each side of Eq. [10] is evaluated separately. In this example, the concentration related terms (the right-hand side of Eq. [10]) give a value of 1.2701×10^{-7} mol/cm^2-s, while the current density related term (the left-hand side of Eq. [10]) gives a value of 1.2707×10^{-7} mol/cm^2-s, when $i_{nj,avg}$ is calculated by Eq. [20]. An incorrect value of 1.2851×10^{-7} mol/cm^2-s is obtained when $i_{nj,avg}$ is calculated by using Simpson's rule applied to Eq. [19].

Table I presents a comparison of various derived quantities of interest obtained from the one-step model with those from the continuous model. The percentage difference between the two methods is high, typically 15-25%, since the conversion per pass is high [Table I shows that approximately 70% of the Cu(I) ions are consumed in a single pass]. However, the one-step method requires substantially less computer time, being on the order of 40 times faster than the continuous model (which consists of 120 axial steps). In systems in which the conversion per pass is low (about 1%), the two methods compare to within 1-5% [see Ref. (12) and (13)]. In Table I, $\lambda_{j,avg}$ is a dimensionless average current density defined as

$$\lambda_{j,avg} = \frac{i_{nj,avg}}{i_{lim,avg}} \qquad [25]$$

where $i_{lim,avg}$ is the average limiting current density of reaction [3] assuming a thin boundary layer (1, 14), and $CPP_{Cu(I)}$ is the fractional conversion per pass of Cu(I) as defined by White et al. (1). That is

$$CPP_i = |\theta_{i,feed} - \theta_{i,avg}(\zeta = 1)| \qquad [26]$$

where $\theta_{i,avg}(\zeta = 1)$ is the average concentration leaving the reactor.

Table II presents a comparison of the calculation of $\lambda_{j,avg}$ obtained by calculating $i_{nj,avg}$ by Eq. [20] with that obtained by using Simpson's rule on Eq. [19]. Note that as the number of axial steps (nk) increases, the method based on Simpson's rule approaches that obtained by using Eq. [20]. Also, at a fixed value of nk, the two methods become equivalent as the driving force E_{cell} decreases, and the current distribution becomes more uniform. The large discrepancy between the two methods, especially at small nk values, is due to the implicit stepping technique itself as well as the assumption in Simpson's rule case that i_{nj} is continuous. In the implicit stepping technique, the first calculated value of i_{nj} is at $x = \Delta x$, not at $x = 0$, so that the end point value ($x = 0$) of $i_{nj}(x)$ required in Simpson's rule must be obtained by an extrapolation, based on the first three calculated values of $i_{nj}(x)$ (8, 13). Table II also shows that for 30 or 60 axial steps, the continuous model behaves more as a series of one-step models because the values of $\lambda_{j,avg}$ calculated when using Eq. [20] have not reached their actual steady value due to the lower accuracy of taking fewer steps. For $nk = 120$ axial

Table I. Comparison of one-step and continuous models

Input parameters[a]
$E_{cell} = 0.6$V
$1/S = 10$ cm^{-1}
$L/v_{avg} = 277.8$s

	One-step	Continuous (120 steps)	% difference from continuous
Δx (cm)	10.0	0.0833	—
$\lambda_{1,avg}$[b]	−0.783	−0.933	16.1
$\lambda_{2,avg}$[b]	0.245	0.230	6.5
$\lambda_{3,avg}$[b]	0.538	0.703	−23.5
$\theta_{Cl^-,avg}(\zeta = 1)$	7.748	9.820	−21.1
$CPP_{Cu(I)}$	0.5398	0.7056	−23.5
$\theta_{Cu(II),avg}(\zeta = 1)$	2.349	2.764	15.0
Computation time on CDC CYBER 170/825 (CPU s)[c]	21.0	892.0	—

[a] See White et al. (1) for the other parameters used in the models.
[b] $\lambda_{j,avg}$ obtained using $i_{nj,avg}$ calculated using Eq. [20].
[c] Central processor unit seconds.

Table II. Comparison of calculation methods for average current density[a]

Number of steps (nk)	E_{cell} (V)	$\lambda_{1,avg}$ *	$\lambda_{1,avg}$ **	$\lambda_{2,avg}$ *	$\lambda_{2,avg}$ **	$\lambda_{3,avg}$ *	$\lambda_{3,avg}$ **
30	0.6	−0.928	−0.950	0.231	0.229	0.697	0.721
60	0.6	−0.931	−0.945	0.231	0.230	0.701	0.715
120	0.6	−0.933	−0.941	0.230	0.230	0.703	0.711
300	0.6	−0.934	−0.938	0.230	0.230	0.704	0.708
120	0.5	−0.817	−0.821	0.184	0.183	0.634	0.638
120	0.4	−0.547	−0.548	0.091	0.090	0.457	0.458

[a] Same input parameters as those in Table I except for E_{cell} as noted.
* $\lambda_{j,avg}$ obtained when $i_{nj,avg}$ calculated using Eq. [20].
** $\lambda_{j,avg}$ obtained when $i_{nj,avg}$ calculated using Simpson's rule on Eq. [19].
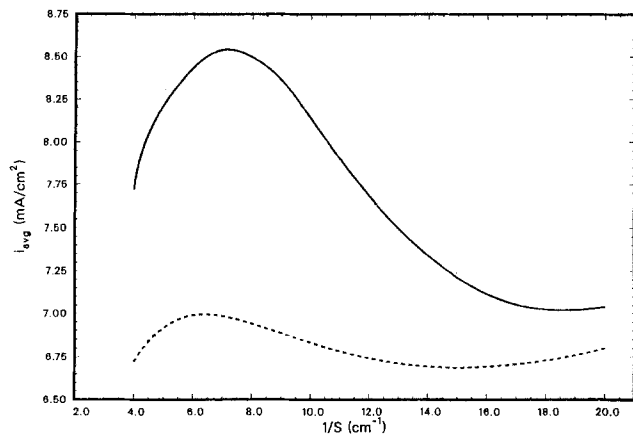
Fig. 4. The effect of electrode surface area per unit volume on the average current density: continuous model (120 axial steps) ——— and one-step model --- (E_{cell} = 0.6V, L/v_{avg} = 277.8s).

Fig. 7. The effect of residence time on the average current density: continuous model (120 axial steps) ——— and one-step model --- (E_{cell} = 0.6V, $1/S$ = 10 cm^{-1}).

steps or greater, the model behaves in a more continuous manner because the value of $\lambda_{j,avg}$ remains relatively unchanged as the number of axial steps is increased. Similar results are obtained for species concentrations and potentials.

Finally, the dependence of the performance of the cell on the independent variables is shown in Fig. 4-9 where

$$CE_{j,avg} = \left| \frac{i_{nj,avg}}{i_{avg}} \right| \qquad [27]$$

and i_{avg} is obtained according to Eq. [25] of Ref. (1) (here $i_{avg} = i_{n1,avg}$ since only one reaction occurs at the anode). Figures 4-9 illustrate for both models the influence of
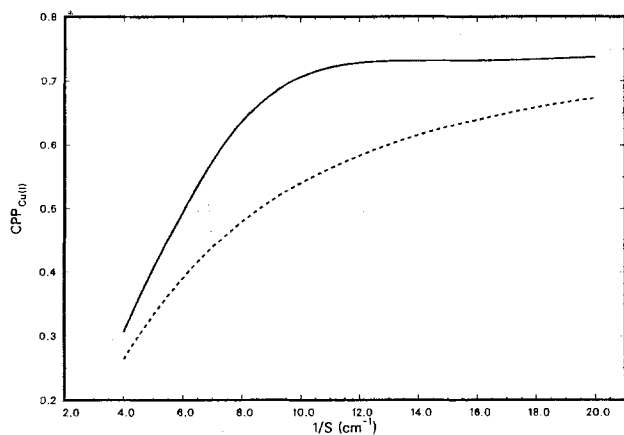

Fig. 5. The effect of electrode surface area per unit volume on Cu(I) conversion per pass: continuous model (120 axial steps) ——— and one-step model --- (E_{cell} = 0.6V, L/v_{avg} = 277.8s).

Fig. 8. The effect of residence time on Cu(I) conversion per pass: continuous model (120 axial steps) ——— and one-step model --- (E_{cell} = 0.6V, $1/S$ = 10 cm^{-1}).

varying $1/S$ or L/v_{avg} while holding fixed E_{cell} and L/v_{avg} or $1/S$, respectively. Figures 4, 5, and 6 present the effect
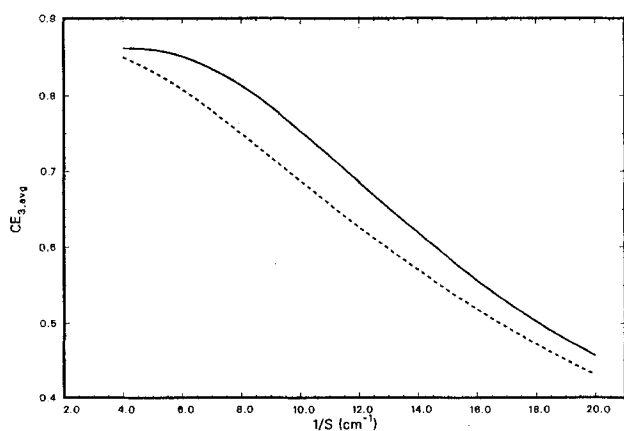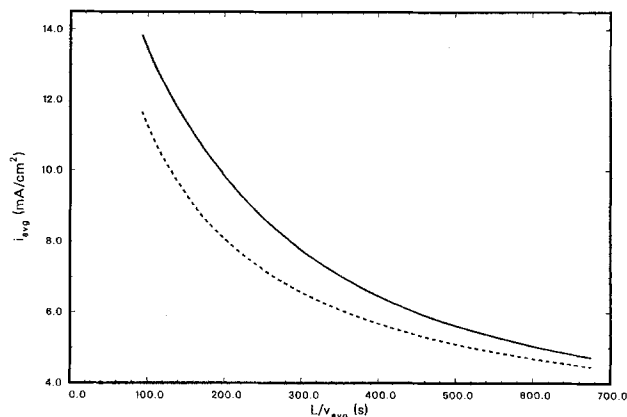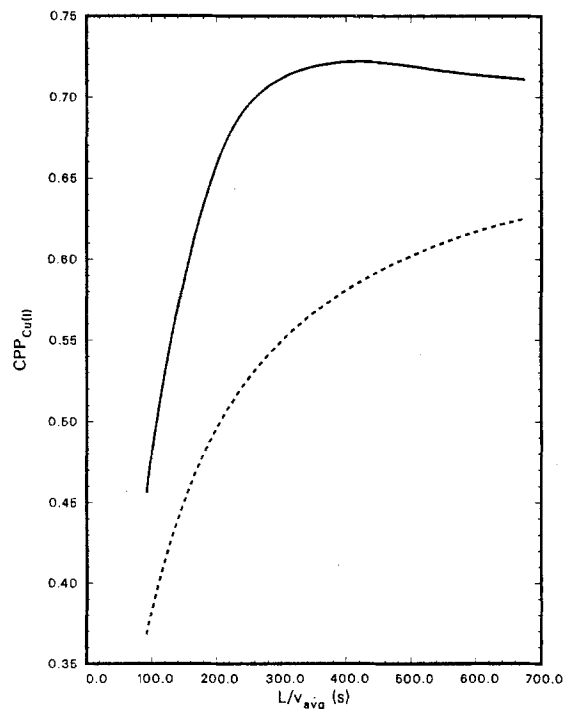

Fig. 6. The effect of electrode surface area per unit volume on the current efficiency for reaction [3]: continuous model (120 axial steps) ——— and one-step model --- (E_{cell} = 0.6V, L/v_{avg} = 277.8s).
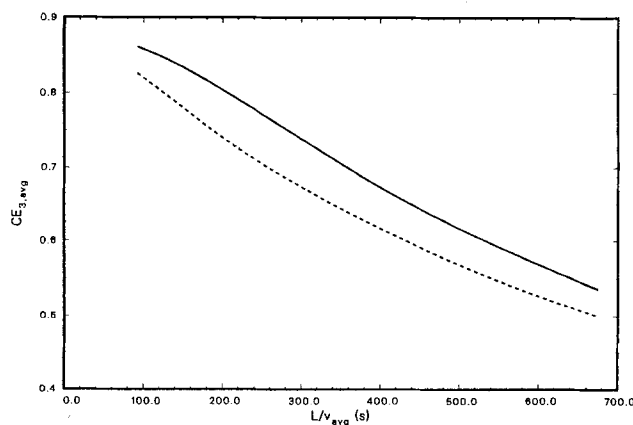

Fig. 9. The effect of residence time on the average current efficiency for reaction [3]: continuous model (120 axial steps) ——— and one-step model --- (E_{cell} = 0.6V, $1/S$ = 10 cm^{-1}).

of varying $1/S$ on i_{avg}, $CPP_{Cu(I)}$ and $CE_{3,avg}$ while holding L/v_{avg} and E_{cell} constant. It is interesting to note, as shown in Fig. 4, that a maximum is predicted in the average current density as function of $1/S$. This maximum is probably due to an increasing i_{avg} due to a lowering of the mass transfer resistance of the cell as $1/S$ is increased below the maximum and a decrease in i_{avg} for values of $1/S$ larger than the maximum due to increasing consumption of the reactant. For values of $1/S$ larger than about 7 cm^{-1}, the current density decreases primarily and the conversion per pass of Cu(I) increases (see Fig. 5). The decrease in $CE_{3,avg}$ shown in Fig. 6 is caused by the lower amount of Cu(I) (as $CuCl_3^{2-}$) available at the cathode due to the high conversion per pass of Cu(I). In addition, the greater amount of $CuCl^+$ that is produced at the anode causes greater amounts of current at the cathode to be consumed by the undesirable reaction 2. Figures 7, 8, and 9 illustrate reactor performance at fixed $1/S$ and E_{cell} while varying the residence time (L/v_{avg}). Note that as the residence time increases, the total reaction rate (shown as i_{avg}) decreases rapidly (Fig. 7). Figure 8 shows that as the residence time increases, Cu(I) reacts more completely, as would be expected, though the continuous model shows the conversion relatively constant after a residence time of about 300s in this example. Finally, Fig. 9 again shows that the current efficiency of reaction 3 ($CE_{3,avg}$) decreases because of lower concentrations of Cu(I) (as $CuCl_3^{2-}$) at the cathode while greater amounts of Cu(II) (as $CuCl^+$) diffuse and migrate to the cathode and are consumed by reaction [2].

Figures 4-9 give a good visual comparison of the one-step model to the continuous model, showing the ability of the one-step method to duplicate the general trends of the continuous model while saving substantial computational costs. Since the predicted reactor performance is similar (though it may actually deviate by up to 25% for large conversion per pass), the one-step model can be used successfully to identify the regions of independent parameter values that produce optimal performance much more rapidly than the continuous model. Once these regions are identified, the continuous model can be used to obtain the desired accuracy of the predicted reactor performance.

Conclusions

This paper shows that for a fixed feed concentration, the selection of $1/S$, L/v_{avg}, and E_{cell} constitute a set of independent parameters which can be used to characterize the performance of a parallel plate electrochemical reactor under laminar flow with a small aspect ratio. The use of these parameters is demonstrated by predicting cell performances by a corrected continuous model and a computationally efficient one-step model.

Acknowledgment

APPENDIX

Material Balance Closure Example

Reactions	j	$\lambda_{j,avg}$ a	$\lambda_{j,avg}$ b	$S_{CuCl_3^{2-},j}$
$CuCl_3^{2-} \rightarrow CuCl^+ + 2Cl^- + e^-$ (anode)	1	−0.933	−0.941	1
$CuCl^+ + 2Cl^- + e^- \rightarrow CuCl_3^{2-}$ (cathode)	2	0.230	0.230	1
$CuCl_3^{2-} + e^- \rightarrow Cu + 3Cl^-$ (cathode)	3	0.703	0.711	−1

$V_a - V_c = 0.6\text{V}$ $nk = 120$ steps
$v_{avg} = 0.036$ cm/s $S = 0.1$ cm $L = 10$ cm
$\mathbf{F} = 96,487$ C/mol $i_{lim,avg} = -8.72 \times 10^{-3}$ A/cm^2
$c_{CuCl_3^{2-},feed} = 0.5 \times 10^{-3}$ mol/cm^3
$c_{CuCl_3^{2-},avg} (x = L) = 0.1472 \times 10^{-3}$ mol/cm^3

species i = $CuCl_3^{2-}$

Left-hand side of Eq. [10]

$$\sum_{j=1}^{nr} \frac{s_{i,j} i_{nj,avg}}{n_j \mathbf{F}} = \frac{i_{lim,avg}}{n \mathbf{F}} \sum_j s_{i,j} \lambda_{j,avg}$$

$$= \frac{-8.72 \times 10^{-3} \text{ A/cm}^2}{(1)(96,487 \text{ C/mol})} [(1)(-0.933) + (1)(0.230)$$

$$+ (-1)(0.703)]$$

$$= 1.2707 \times 10^{-7} \frac{\text{mol}}{\text{cm}^2\text{s}}$$

(by using Eq. [20] to determine $i_{nj,avg}$)

$$= 1.2851 \times 10^{-7} \frac{\text{mol}}{\text{cm}^2\text{s}}$$

(by using Simpson's rule for $i_{nj,avg}$ according to Eq. [19]).

Right-hand side of Eq. [10]

$$[c_{i,feed} - c_{i,avg}(x = L)] \frac{v_{avg} S}{L}$$

$$= (0.5 - 0.1472) \times 10^{-3} \frac{\text{mol}}{\text{cm}^3} \frac{(0.036 \text{ cm/s})(0.1 \text{ cm})}{10 \text{ cm}}$$

$$= 1.2701 \times 10^{-7} \frac{\text{mol}}{\text{cm}^2\text{s}}$$

Thus, the two sides of Eq. [10] are equal within calculational accuracy if Eq. [20] is used to determine $i_{nj,avg}$.

---

[a] $\lambda_{j,avg}$ obtained when $i_{nj,avg}$ calculated by Eq. [20].
[b] $\lambda_{j,avg}$ obtained when $i_{nj,avg}$ calculated using Simpson's rule on Eq. [19].

LIST OF SYMBOLS

c_i — concentration of species i, mol/cm^3
c_{io} — concentration of species i at the electrode surface, mol/cm^3
$c_{i,avg}$ — average concentration of species i at a particular axial position, mol/cm^3
$c_{i,feed}$ — feed concentration of species i, mol/cm^3
$c_{i,ref}$ — fixed reference concentration of species i, mol/cm^3
$CE_{j,avg}$ — average current efficiency for reaction j
CPP_i — fractional conversion per pass of species i
D_i — diffusion coefficient of species i, cm^2/s
D_R — diffusion coefficient of limiting reactant, cm^2/s
E_{cell} — applied cell potential (=$V_a - V_c$), V
$\mathbf{F}$ — Faraday's constant, 96,487 C/mol
i_{avg} — average current density at an electrode (= $\sum_j i_{nj,avg}$ for all reactions at a particular electrode), A/cm^2
$i_{lim,avg}$ — average limiting current density, as given in White *et al.* (1), A/cm^2
i_{nj} — normal component of current density due to reaction j, A/cm^2
$i_{nj}(k)$ — the value of i_{nj} on the kth reactor segment length, A/cm^2
$i_{nj,avg}$ — average normal current density due to reaction j, A/cm^2
$i_{oj,ref}$ — exchange current density of reaction j evaluated at reference concentrations, A/cm^2
k — integer counter of axial steps in solution technique
L — electrode length, cm
L/v_{avg} — residence time of the reactor, s
N_{fi} — flux of species i in the flow direction (x direction), mol/cm^2-s
n_j — number of electrons passed in reaction j
N_{ni} — normal component of the flux (y direction) of species i, mol/cm^2-s
nk — number of steps taken along the electrode length in solution technique
p_{ij} — anodic reaction order of species i in reaction j, see White *et al.* (1)
Pe — Peclet number (=$2Sv_{avg}/D_R$)
q_{ij} — cathodic reaction order of species i in reaction j, see White *et al.* (1)
R — gas law constant, 8.314 J/mol-K
S — total electrode gap, cm
$1/S$ — equals surface area of an electrode per unit of cell volume, cm^{-1}
s_{ij} — stoichiometric coefficient of species i in reaction j
T — temperature, K

V_a	anode potential, V
v_{avg}	average velocity of the electrode, cm/s
V_c	cathode potential, V
v_x	velocity component of the electrolyte in the x-direction, cm/s
W	width of the electrode, cm
x	axial coordinate, cm
y	radial coordinate, cm
z_i	charge number of species i

Greek

α	aspect ratio, S/L
β_{ij}	dimensionless residence time
Δx	axial step size, cm
ζ	dimensionless axial coordinate (x/L)
η	dimensionless axial coordinate (y/S)
θ_i	dimensionless concentration of species i $(c_i/c_{i,ref})$
$\theta_{i,avg}$	dimensionless average concentration of species i
$\theta_{i,feed}$	dimensionless feed concentration of species i
$\theta_{i,o}$	dimensionless concentration of species i at the electrode surface
$\lambda_{j,avg}$	the ratio of average current density for reaction j to the average limiting current density $(i_{nj,avg}/i_{lim,avg})$
ξ_{ij}	dimensionless formulation of the electrode gap
Φ	solution potential, V

REFERENCES

1. R. E. White, M. Bain, and M. Raible, *This Journal*, **130**, 1037 (1983).
2. G. P. Sakellaropoulos, *AIChE J.*, **25**, 781 (1979).
3. G. P. Sakellaropoulos and G. A. Francis, *This Journal*, **126**, 1928 (1979).
4. G. P. Sakellaropoulos and G. A. Francis, *J. Chem. Tech. Biotechnol.*, **30**, 102 (1980).
5. W. R. Parrish and J. S. Newman, *This Journal*, **117**, 43 (1970).
6. R. Caban and T. W. Chapman, *ibid.*, **123**, 1036 (1976).
7. J. Lee and J. R. Selman, *ibid.*, **129**, 1670 (1982).
8. B. Carnahan, H. A. Luther, and J. O. Wilkes, "Applied Numerical Methods," John Wiley & Sons, Inc., New York (1969).
9. J. S. Newman, "Electrochemical Systems," Prentice-Hall, Inc., Englewood Cliffs, NJ (1973).
10. R. E. White, *Ind. Eng. Chem. Fundam.*, **17**, 367 (1978).
11. T. V. Nguyen, C. W. Walton, R. E. White, and J. Van Zee, *This Journal*, **133**, 81 (1986).
12. M. Mader and R. E. White, *ibid.*, In press.
13. M. Mader, M.S. Thesis, Texas A&M University, College Station, TX (1985).
14. W. R. Parrish and J. Newman, *This Journal*, **116**, 169 (1969).

A Mathematical Model for a Parallel Plate Electrochemical Reactor, CSTR, and Associated Recirculation System

T. V. Nguyen,* C. W. Walton,* and R. E. White**

Department of Chemical Engineering, Texas A&M University, College Station, Texas 77843

ABSTRACT

A mathematical model is presented for a system comprised of a parallel plate electrochemical reactor (PPER) and a continuous, stirred-tank reactor (CSTR) under both total and partial recycle. The model is used to predict the time dependent behavior of the electrowinning of copper from an aqueous, hydrochloric acid solution. The model includes many important aspects of a PPER/CSTR system which have been neglected previously. These aspects are the kinetics of electrode reactions, the electroneutrality condition, three mass transfer processes for ionic species in the electrolyte (diffusion, ionic migration, and convection) and the electrode gap in the PPER, and the inclusion of a true CSTR in the recycle stream.

Parallel plate electrochemical reactors have been used in many industrial electrochemical processes: chlor-alkali production, metal extraction and refining, and electro-organic synthesis, as well as in batteries and fuel cells (1, 2). In some of these processes, the system consists of a parallel plate electrochemical reactor (PPER), a continuous, stirred-tank reactor (CSTR), and an associated recirculation system, as shown in Fig. 1 and 2. The CSTR plays a very important role in some electrochemical processes in which the electrochemical reactor is used mainly to generate the necessary reactants that produce the final product through homogeneous chemical reactions in the CSTR. An example of such a process is the electrogeneration of hypochlorite and chlorate (3-8). There have been several models developed for a PPER in total recycle with a well-mixed reservoir in which the PPER was treated as a plug flow reactor (9, 10) or a plug flow reactor with axial diffusion (11). No model for a batch PPER system was found which includes in the PPER the effects of the separation of the electrodes, applied cell potential, ionic migration, and the kinetics of the electrode reactions, and in the well-mixed reservoir, the capability of handling chemical reactions.

Pickett (9, 12) presented simple approximate models in which the electrochemical reactor is considered to be an ideal plug flow reactor operating at limiting current conditions for a single reaction. To obtain his analytical solutions, Pickett decoupled the governing equations for the PPER from those of the reservoir by assuming that the residence time in the reservoir is large enough to ignore the time dependence of the outlet concentration of the reservoir (which, of course, is the same as the feed concentration to the electrochemical reactor). Thus, his models are applicable only to a process with a very large residence time in the reservoir. Mustoe and Wragg (11) presented an approximate model similar to those of Pickett, but extended the transport equation for the
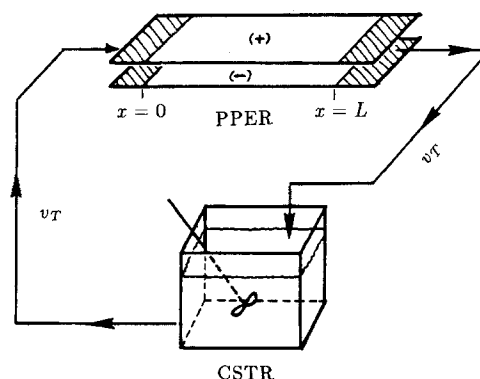

Fig. 1. Schematic of a batch PPER/CSTR or reservoir system